

## *International Journal of Scientific Research and Reviews*

### **Study of Carbazole Based Dyes for Dye Sensitized Solar Cells: Effect of Different Linker Groups for Dye-Sensitised Solar Cells.**

**Anjali Pandey\*, Ashutosh kumar and Anil Mishra**

Department of Chemistry, University of Lucknow, Lucknow 226007, India

#### **ABSTRACT**

Novel metal free carbazole based organic dyes were designed utilizing different linker group and understand their roles in dye-sensitized solar cells (DSSCs). The linker groups which were studied are 3,4-ethylene dioxythiophene (D 1), oxadiazole (D 2), quinoxaline (D 3) and thio[3,4-b] pyrazene (D 4). It has been investigated theoretically with density functional theory (DFT) calculation at hybrid functional B3LYP by using 6-31+ G\*\* to evaluate the effects of various linker groups on the optical and electronic properties of the dyes in dye-sensitised solar cells. Optical properties were calculated using the time-dependent DFT calculations with the B3LYP and coulomb-attenuating method CAM-B3LYP. Optical and electronic properties, UV-Vis absorption spectra, light harvesting efficiency of the dyes have been studied to shed light on how the various linker groups influence the properties of the dyes. The dyes served as efficient sensitizers in DSSCs owing to their promising optical and electrochemical properties.

**KEYWORDS** – DSSCs, carbazole, optical properties, DFT Method, NLO Properties.

#### **\*Corresponding author**

**Anjali Pandey**

Department of Chemistry,  
University of Lucknow,  
Lucknow 226007, India

## 1. INTRODUCTION

In the current scenario, dye sensitized solar cells (DSSCs) have attracted much attention due to their potential advantages of low cost, environment friendliness, flexibility, transparency relative to conventional crystalline silicon solar cells<sup>1</sup> and high power conversion efficiency (PCE), as reported by O'Regan and Gratzel in 1991.<sup>2</sup> Metal-free dyes have advantageous as compared with other dyes for DSSCs due to their flexibility in molecular design and low production cost.<sup>3,4,5,6</sup> Metal free dyes can be synthesized easily and economically. They show high molar extinction coefficients due to intermolecular  $\pi - \pi^*$  transitions. Generally organic dyes (use as sensitizer) contain D- $\pi$ -A structure, where D is donor,  $\pi$  is linker and A is acceptor.<sup>7</sup>

The efficiency of organic dyes in DSSCs vary with chemical modification due to their tuned redox and absorption properties.<sup>8</sup> Organic dyes used in DSSCs must have appropriate levels for the lowest unoccupied molecular orbital (LUMO) and the highest occupied molecular orbital (HOMO) of the dye matching the CB edge level of the TiO<sub>2</sub> and the iodine redox potential, respectively. The energy level of the LUMO of the dye must be higher than the CB of the TiO<sub>2</sub> (-4.1 eV), and the energy level of the HOMO of the dye must be lower than the I<sup>-</sup>/I<sub>3</sub><sup>-</sup> redox potential (-4.80 eV).<sup>9,10,11</sup> By changing the electron donor, acceptor or  $\pi$ -spacer group of organic dyes, the HOMO and LUMO energy levels and also absorptivities and electronic excitation energies of the dyes can be changed.<sup>12</sup> Carbazole-based organic materials have been widely employed as active constituent in electronic devices such as organic light-emitting diodes (OLEDs)<sup>13</sup> and DSSCs<sup>14</sup> due to their unique charge transporting properties and pronounced thermal stability. Carbazole is an attractive building block as it offers many nuclear sites for functional group incorporation.<sup>15,16</sup> Particularly, in the dyes serving as sensitizers in DSSCs, carbazole has been used either as a peripheral donor.<sup>17</sup> Due to the presence of electron rich amine functionality, carbazole can easily donate electron; however, the cation radical formed after the removal of electron is quite unstable owing to the large structural reorganization associated with the oxidation. Substitution of electron releasing groups on the contrary on the carbazole nucleus can enhance the donor strength of the carbazole.<sup>18,19</sup> Keeping all this in mind, we have designed and synthesized a series of metal free organic dyes containing carbazole as a donor. Attempts to increase the performance of organic dyes not only in the synthesis laboratory, but also in the field of theoretical investigation based on computational study have been undertaken by several investigators for understanding the mechanism of electron transfer.<sup>20,21</sup>

In this paper, we studied newly designed series of metal free carbazole based organic dyes which were comprehensively investigated by computational methods, in order to understand the

roles of 3,4-ethylene dioxythiophene (D1), oxadiazole (D 2), quinoxaline (D 3) and thio[3,4-b] pyrazene (D 4) as the linker groups in dye-sensitized solar cells (DSSCs). Optical and electronic properties, UV-Vis absorption spectra, MESP, ESP, light harvesting efficiency, have been studied to shed light on how the various anchoring groups influence the properties of the dyes. The molecular structure and IUPAC name of dyes are given in figure 1

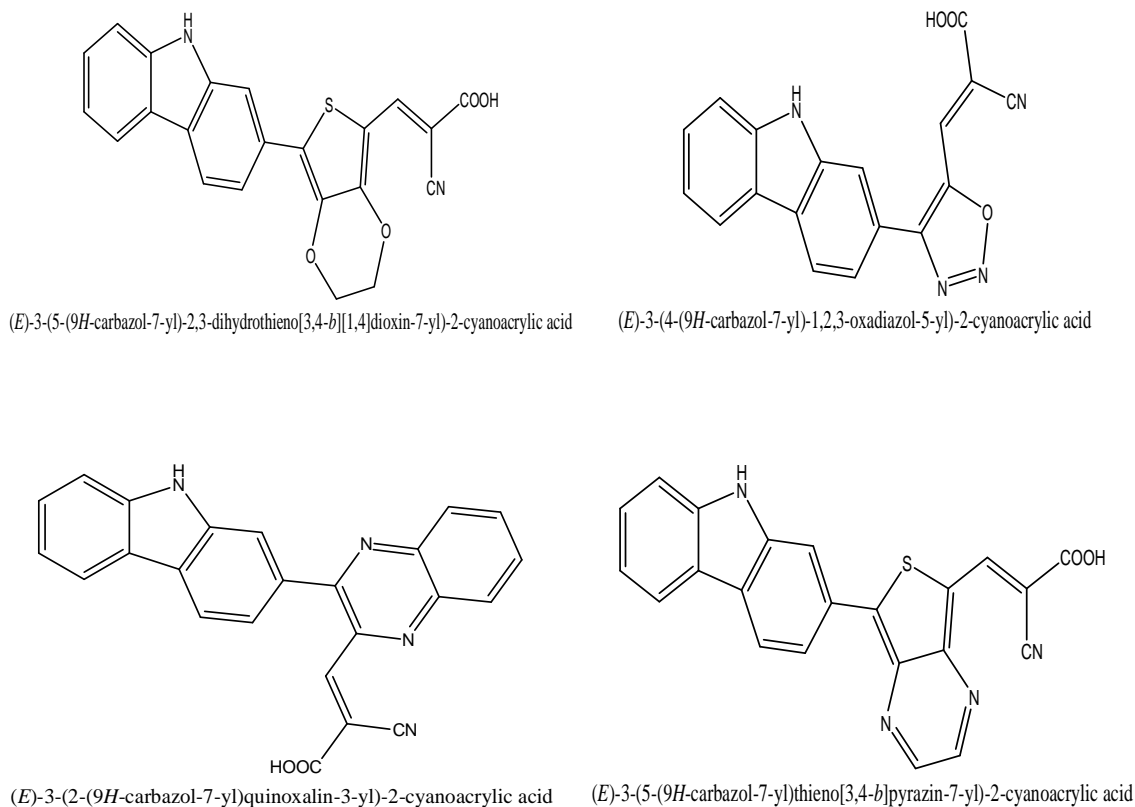


**Figure 1. Molecular structure and IUPAC names of dyes 1-4**

## 2. MATERIALS AND METHOD COMPUTATIONAL METHOD

All the geometries of dyes have been fully optimized using the B3LYP method within the framework of density functional theory (DFT) in conjunction with the 6-31+G\*\* basis set i.e., Becke's three parameters non-local hybrid exchange potential with the non-local correlation functional of Lee, Yang and Parr (B3LYP)<sup>22,23</sup> in the gas phase.

The absorption spectra, excitation energies and oscillator strengths of the were used to calculate the light harvesting efficiency (LHE) by TDDFT calculations. The conductor polarisable continuum model (CPCM) is used to calculate the solvent effects.<sup>24</sup> All these calculations were performed using GAUSSIAN 09 program package

### 3. RESULTS AND DISCUSSION MOLECULAR GEOMETRY AND ENERGY

The optimized structure of dyes were in the ground state using DFT at the B3LYP/6-31G(d,p) level of theory is shown in Fig.2 The Global Minimum Energies obtained for the optimized structures of dyes are presented in Table 1.

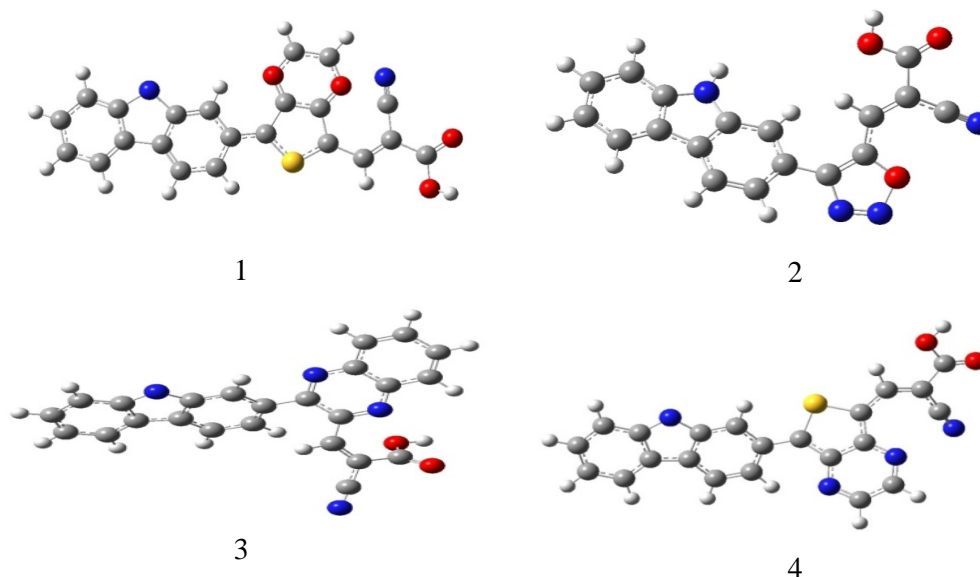


Figure 2. Optimized geometries of dyes 1- 4 in THF with B3LYP/6-31+G\*\*

Table 1. Global minimum energies, (a.u) of dyes 1- 10

Dyes	Global minimum energy (a.u)
Dye 1	-1653.81
Dye 2	-1136.85
Dye 3	-1292.78
Dye 4	-1613.54

### ELECTRONIC ABSORPTION

The excitation energies, wavelengths and transition probabilities (oscillator strengths) of the dyes were computed in TD-DFT method using B3LYP and 6-31-G(d,p) basis sets and solvent effect has been taken into account by employing the conductor polarisable continuum model (CPCM). The  $E_{\text{HOMO}}$ ,  $E_{\text{LUMO}}$  and HOMO-LUMO gap (HLG) ( $E_{\text{LUMO}} - E_{\text{HOMO}}$ ) of these dyes are reported in Table: 2 for gas phase as well as in THF. Bar graph showing the energy of HOMO –LUMO and their Energy Gap of all dyes in gas phase is given in figure: 3. The  $E_{\text{HOMO}}$  and  $E_{\text{LUMO}}$  for these dyes in the two phases are in increasing order: gas < THF, while the values of HLG for these dyes are in the opposite order. Calculated results show that the HOMO energy levels of these dyes are lower than the reduction potential energy of the  $\Gamma/\Gamma_3$  electrolyte ( $-4.8$  eV), i.e. these dyes that lose electrons

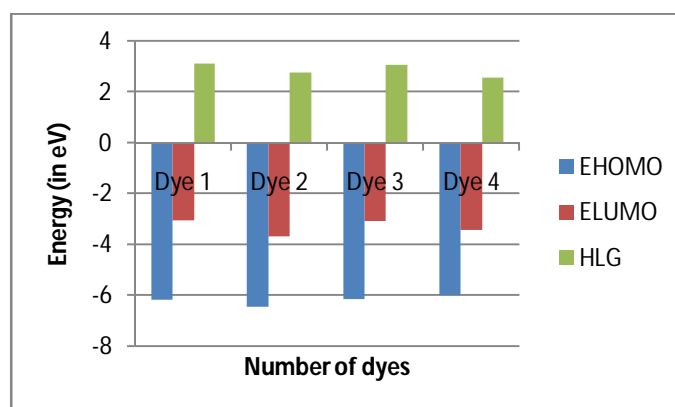
could be restored by getting electrons from the electrolyte, and, the LUMO energy levels of these dyes are higher than the TiO<sub>2</sub> CB edge (-4.1 eV).<sup>25</sup> This shows that the LUMO levels of all dyes should be capable of injecting electrons into the CBs of TiO<sub>2</sub>.

**Table 2. E<sub>HOMO</sub>(eV), E<sub>LUMO</sub>(eV) HLG(eV) and maximum wavelength ( $\lambda_{\max}$ ) of dyes. In gas phase**

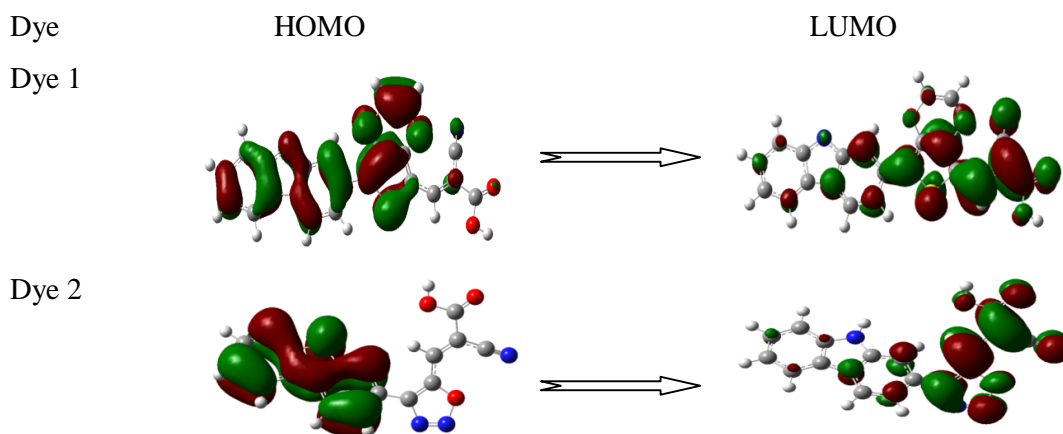
Dye	E <sub>HOMO</sub>	E <sub>LUMO</sub>	HLG	$\lambda_{\max}^a$	Main transition
Dye 1	-6.171	-3.068	3.103	408.43	H→L(81.16%)
Dye 2	-6.453	-3.698	2.755	324.83	H→L(70.45%)
Dye 3	-6.164	-3.101	3.063	473.84	H→L(70.29%)
Dye 4	-6.020	-3.456	2.564	536.49	H→L(69.40%)

In thf

Dye	E <sub>HOMO</sub>	E <sub>LUMO</sub>	HLG	$\lambda_{\max}^a$	Main transition
Dye 1	-6.086	-3.104	2.982	439.12	H→L(76.19%)
Dye 2	-6.189	-3.665	2.524	248.28	H→L(70.48%)
Dye 3	-7.461	-1.981	5.479	334.33	H→L(46.71%)
Dye 4	-6.003	-3.444	2.559	559.51	H→L(59.26%)



**Figure 3. Bar graph showing the energy of HOMO –LUMO and their Energy Gap of dyes in gas phase**



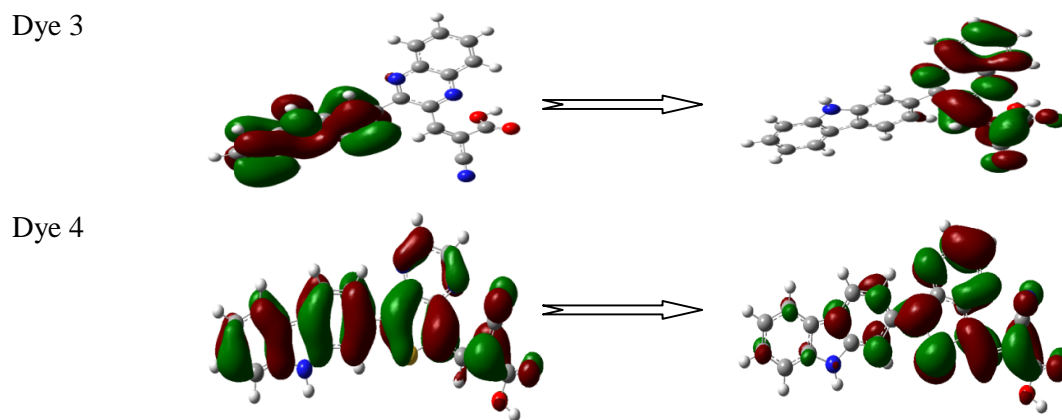


**Figure 4. The distribution patterns of FMOs of Dye 1-4**

TDDFT excited state calculations with the B3LYP/6-311+G\*\*, based on the optimised geometries of B3LYP/6-311+G\*\*, were carried out on the 20 lowest singlet-singlet transitions for the dyes in the gas phase and the solvent. The results in Table 2 show that the presence of solvent shifts the absorption bands of these dyes toward the longer wavelength. Because in these electronic transitions, with increasing solvent polarity, the energy of the excited state is lowered more than that of the ground state, and this produces a red shift. It means that the better stabilisation of the  $\pi^*$  relative to the  $\pi$  with the inclusion of solvent will result in a red shift. The HLG of these dyes in THF is smaller than that in vacuum, consequently it induces a red shift of the absorption as compared with that in vacuum. The simulated absorption spectra by B3LYP in THF for all the dyes are shown in Figure 4.

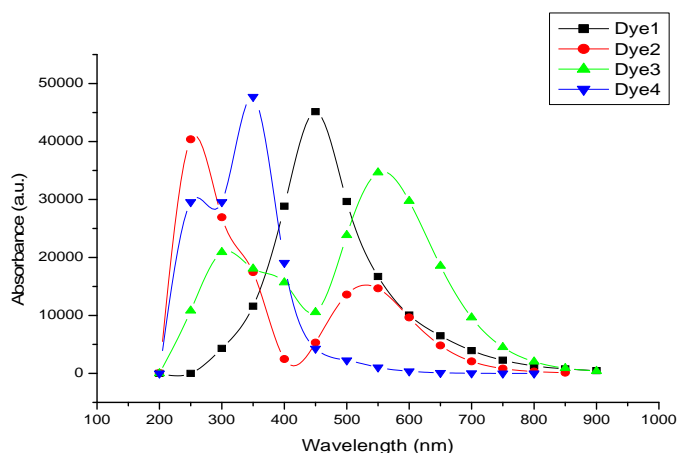


**Figure 4. Electronic absorption spectra of dyes 1-4 in the solvent (THF) with B3LYP/6-311+G\*\***

The visible and near UV regions are the most important region for photon-to-current conversion to obtain the microscopic information about the electronic transitions and its corresponding MO properties. The efficiency of electron injection could influence

the short-circuit photocurrent density ( $J_{sc}$ ) that is a key factor affecting the efficiency of DSSCs. The singlet to singlet transitions of the absorption bands with maximum wavelength and oscillator strength are listed in table. 3. Light-harvesting efficiency  $LHE(\lambda)$  of a dye which is a factor related to  $J_{sc}$ , the LHE of the dye sensitizer should be as high as possible to maximize the photocurrent response and can be quantified by the following equation:

$$LHE = 1 - 10^{-A} = 1 - 10^{-f} \quad (1)$$

where  $f$  is the oscillator strength of the dye associated with the wavelength corresponding to the peak absorbance through intramolecular charge transfer.<sup>26,27</sup>

**Table 3. Calculated  $\lambda_{max}$  (nm), oscillator strengths ( $f$ ), light-harvesting efficiency (LHE) of the dyes at the B3LYP/6-311+G\*\* level**

Dyes	$\lambda_{max}$ (nm)	$f$	LHE
Dye 1	439.12	0.985	0.896
Dye 2	248.28	0.785	0.835
Dye 3	334.33	0.555	0.721
Dye 4	559.51	0.541	0.712

## GLOBAL REACTIVITY PARAMETERS

### 1. Chemical potential ( $\mu$ )

Parr, Donnelly, Levy and Palke established the basic relationship of the density functional theory of chemical reactivity.<sup>28</sup> They linked the chemical potential of DFT with the first derivative of the energy with respect to the number of electrons. They therefore, linked the chemical potential ( $\mu$ ) with the negative of the electronegativity  $\chi$

$$\mu = -\chi \quad 1$$

### 2. Ionization Potential ( $I$ )

Koopman's theorem states that,<sup>29</sup> ionization potential ( $I$ ) may be defined in terms of the energy of the HOMO and the LUMO. Ionization potential ( $I$ ) is defined as the amount of energy required to remove an electron from a molecule. It is related to the energy of the  $E_{HOMO}$  through the equation:

$$I = -E_{HOMO} \quad 2$$

### 3. Electron Affinity ( $A$ )

Koopman's theorem also states that,<sup>30</sup> Electron affinity ( $A$ ) may also be defined in terms of the energy of the HOMO and the LUMO. Electron affinity ( $A$ ) is defined as the energy released when a proton is added to a system.<sup>41</sup> It is related to  $E_{LUMO}$  through the equation:

$$A = -E_{LUMO} \quad 3$$

4. Electronegativity ( $\chi$ )

One can determine the electronegativity,  $\chi$ , when the values of  $I$  and  $A$  are known. As it is defined as the measure of the power of an atom or group of atoms to attract electrons towards itself.<sup>31</sup> It can be represented by the equation:

$$\chi = (I + A)/2 \quad 4$$

The above reactivity descriptors have been calculated using equations. [(1) - (4)] and listed in table 4.

**Table 4.** Calculated  $E_{\text{HOMO}}$ (eV),  $E_{\text{LUMO}}$ (eV), chemical potential ( $\mu$ ), ionization potential (I), electron affinity (A), electronegativity ( $\chi$ ) using DFT/B3LYP/6-31G(d,p)

Dye	$E_{\text{HOMO}}$	$E_{\text{LUMO}}$	Chemical potential ( $\mu$ )	Ionization Potential (I)	Electron Affinity (A)	Electro negativity ( $\chi$ )
Dye 1	-6.171	-3.068	-4.619	6.171	3.068	4.619
Dye 2	-6.453	-3.698	-5.075	6.453	3.698	5.075
Dye 3	-6.164	-3.101	-4.632	6.164	3.101	4.632
Dye 4	-6.020	-3.456	-4.738	6.020	3.456	4.738

## NON -LINEAR OPTICAL ANALYSIS

Non linear optics (NLO) is an important concept in determining the optical and electronic properties of any molecule. It is difficult to measure the hyperpolarizability directly. So it is advisable to choose computational method (DFT) for its calculation as it is a good alternative based on finite field approach. DFT has been widely used as an effective method to study the organic NLO materials. Dipole moment, polarisability and hyperpolarisability are important physical quantities of dye sensitizer that could be affected by changing molecular structure.<sup>32</sup>

Polarisabilities are nonlinear optical (NLO) properties which in turn determine intramolecular charge delocalisation in  $\pi$ -electron-conjugated dyes. It has been accepted that dye sensitizer with high NLO properties, usually have high photoelectric conversion efficiency.<sup>33,34</sup>

The theoretical calculations of the dipole moment ( $\mu$ ), mean linear polarizability ( $\alpha$ ), anisotropy of polarizability ( $\Delta\alpha$ ) and the first order hyperpolarizability ( $\beta$ ) is done using the following equations:

The dipole moment could be calculated with the following formula:

$$\mu = \sqrt{\mu_x^2 + \mu_y^2 + \mu_z^2} \quad (5)$$

where  $\mu_x$ ,  $\mu_y$ ,  $\mu_z$  are defined as the vector components of the dipole moment.

The definition of the isotropic polarisability,  $\alpha$ , and the anisotropy of polarisability,  $\Delta\alpha$ , are as Equations (3) and (4), respectively. In these equations,  $\alpha_{xx}$ ,  $\alpha_{yy}$ ,  $\alpha_{zz}$  are the tensor components of polarisability

$$\alpha = \frac{(\alpha_{xx} + \alpha_{yy} + \alpha_{zz})}{3} \quad (6)$$

$$\Delta\alpha = \sqrt{\left[ \frac{(\alpha_{xx} - \alpha_{yy})^2 + (\alpha_{xx} - \alpha_{zz})^2 + (\alpha_{yy} - \alpha_{zz})^2}{2} \right]} \quad (7)$$

The total first-order hyperpolarisability,  $\beta_{tot}$ , is defined as:

$$\beta_{tot} = \sqrt{\left[ (\beta_{xxx} + \beta_{xyy} + \beta_{xzz})^2 + (\beta_{yyy} + \beta_{xzz} + \beta_{yxx})^2 + (\beta_{zzz} + \beta_{zxx} + \beta_{zyy})^2 \right]} \quad (8)$$

where  $\beta_{xxx}$ ,  $\beta_{xyy}$ ,  $\beta_{xzz}$ ,  $\beta_{yyy}$ ,  $\beta_{yxx}$ ,  $\beta_{yzz}$ ,  $\beta_{yxx}$ ,  $\beta_{zzz}$ ,  $\beta_{zxx}$  and  $\beta_{zyy}$  are the tensor components of hyperpolarisability.

Table 5.a. Calculated dipole moment  $\mu$  (Debye)

Dye	$\mu_x$	$\mu_y$	$\mu_z$	M
Dye 1	6.7037	-3.7609	-3.1240	8.2972
Dye 2	-8.7739	3.9829	0.7489	9.6647
Dye 3	-1.8272	-7.4009	1.4531	7.7604
Dye 4	-8.0320	-3.0438	-3.0290	9.1078

Table 5.b. Calculated isotropic polarisability  $\alpha$  and anisotropy of polarisability  $\Delta\alpha$

Dye	$\alpha_{xx} (10^3)$	$\alpha_{yy} (10^3)$	$\alpha_{zz} (10^3)$	$\alpha (10^{-22} \text{ esu})$	$\Delta\alpha (10^{-22} \text{ esu})$
Dye 1	0.750794	0.305851	0.160032	0.600	0.789
Dye 2	0.497807	0.271988	0.137025	0.447	0.467
Dye 3	0.551601	0.390865	0.181597	0.555	0.476
Dye 4	0.778144	0.333162	0.166276	0.631	0.811

Table 5.c. Calculated total first-order hyperpolarisability  $\beta_{tot}$

Dye	$\beta_{xxx}$	$\beta_{xxy}$	$\beta_{xyy}$	$\beta_{yyy}$	$\beta_{xxz}$	$\beta_{yyz}$	$\beta_{xzz}$	$\beta_{zzz}$	$\beta_{tot}(10^{-28} \text{ esu})$
Dye 1	-6588.61	-1454.8	346.25	-598.32	325.23	158.96	136.62	-40.15	0.556
Dye 2	10500.4	948.47	647.28	384.84	183.45	119.92	-103.988	56.83	0.962
Dye 3	4956.92	49.57	349.17	628.57	-73.36	-138.17	18.18	59.90	0.464
Dye 4	17809.3	1133.1	775.08	-17.44	-172.99	-34.85	-115.48	18.35	1.59

## CONCLUSION

In this study four novel carbazole based organic dyes with different anchoring groups have been investigated by DFT and TDDFT methods to evaluate the effects of various anchoring groups on the electronic and optical properties, electron injection efficiency and also the CB shift of  $\text{TiO}_2$  due to the adsorption of these dyes onto the surface.

The factors, including maximum absorption wavelength ( $\lambda_{\text{max}}$ ), light-harvesting efficiency (LHE), dipole moment ( $\mu$ ), the NLO properties (polarisability ( $\alpha$ ), anisotropy of polarisability ( $\Delta\alpha$ ) and hyperpolarisability ( $\beta$ )) of all the dyes, have been calculated by computational methods. The influences of different anchoring groups on these factors demonstrate that dyes 1 with 3,4-ethylene dioxythiophene as the linker groups in dye-sensitized solar cells (DSSCs), have the best absorption properties, i.e. the high  $\lambda_{\text{max}}$ , largest HOMO-LUMO gap, the widest absorption spectrum, the largest LHE. Also, have high NLO properties. Above study will be useful for the design of organic dyes with target properties to increase the efficiency of DSSCs.

## **ACKNOWLEDGEMENT**

The authors convey their profound thanks to the Head, Department of Chemistry, University of Lucknow, Lucknow, for providing laboratory facilities and central facility for computational research.

## **REFERENCE**

1. Gratzel M, Dye-sensitized solar cells. *J. Photo chem. Photobiol. C* 4, 2003; 145–153.
2. O'Regan B, Gratzel M. A low-cost, high-efficiency solar cell based on dye-sensitized colloidal TiO<sub>2</sub> films. *Nature*, 1991; 353: 737–740.
3. Ning Z, Fu Y, Tian H. Improvement of dye-sensitized solar cells: what we know and what we need to know. *Energy Environ. Sci.*, 2010; 3: 1170–1181,.
4. Zhang M, Wang Y, Xu M, Ma W, Li R, Wang P. Design of high-efficiency organic dyes for titania solar cells based on the chromophoric core of cyclopentadithiophene-benzothiadiazole *Energy Environ Sci.* 2013; 6: 2944–2949.
5. Huang Z S, Feng H L, Zang X F, Iqbal Z, Zeng HP, Kuang DB, Wang LY, Meier H, Cao DR. Phenothiazine-based dyes for efficient dye-sensitized solar cells *J. Mater. Chem. A*, 2014; 2: 15365– 15376.
6. Chen YC, Chen YH, Chou HH, Chaurasia S, Wen YS, Lin JT, Yao CF. Naphthyl and thienyl units as bridges for metal-free dye-sensitized solar cells. *Chem.–Asian J.* 2012; 7: 1074–1084.
7. Singh SP, Roy MS, Thomas KRJ, Balaiah S, Bhanuprakash K, Sharma GD. New Triphenylamine Based Organic Dyes with Different Numbers of Anchoring Groups for Dye-Sensitized Solar Cells. *J. Phys. Chem. C*, 2012; 116: 5941–5950.
8. Zhang J, Kan YH, Li HB, Geng Y, Wu Y, Su ZM. How to design proper  $\pi$ -spacer order of the D- $\pi$ -A dyes for DSSCs? A density functional response Dyes Pigments. 2012; 95: 313-321.
9. Mikroyannidis JA, Tsagkournos DV, Balraju P, Sharma GD. Low band gap dyes based on 2-styryl-5-phenylazo-pyrrole: Synthesis and application for efficient dye-sensitized solar cells *J. Power Sources* 2011; 196: 4152.

10. Kotchaprastit P, rachumrak N, Tarsang R, Jungstittiwong S, Keawin T, Sudyoasuk T, Promarak V. Pyrene-Functionalized Carbazole Derivatives as Non-Doped Blue Emitters for Highly Efficient Blue Organic Light-Emitting Diodes. *J. Mater. Chem. C*. 2013; 1: 4916-4924.
11. Ooyama Y, Inoue S, Nagano T, Kushimoto K, Ohshita J, Imae I, Komaguchi K, Harima Y. Dye-Sensitized Solar Cells Based On Donor-Acceptor  $\pi$ -Conjugated Fluorescent Dyes with a Pyridine Ring as an Electron-Withdrawing Anchoring Group. *Angew. Chem., Int. Ed.*, 2011; 50: 7429-7433.
12. Wang HY, Liu F, Xie LH, Tang C, B Peng, Huang W, Wei W. Topological Arrangement of Fluorenyl-Substituted Carbazole Triads and Starbursts: Synthesis and Optoelectronic Properties. *J. Phys. Chem. C*, 2011; (115) 6961-6967.
13. Huang H, Fu Q, Pan B, Zhuang S, Wang L, Chen J, Ma D, Yang C. Butterfly-Shaped Tetrasubstituted Carbazole Derivatives as a New Class of Hosts for Highly Efficient Solution-Processable Green Phosphorescent Organic Light-Emitting Diodes. *Org. Lett.* 2012; 14: 4786-4789.
14. Venkateswararao A, Thomas KRJ, Tiwari A, Boukherroub R, Sharon M, Beverly MA, Eds.; Wiley-Scrivener: In *Solar Cell Nanotechnology*; Chapter, 2014; 2: 41-96.
15. Teng C, Yang X, Li S, Cheng M, Hagfeldt A, Wu L, Sun L. Tuning the HOMO Energy Levels of Organic Dyes for Dye-Sensitized Solar Cells Based on  $\text{Br}^-/\text{Br}^{3-}$  Electrolytes. *Chem. Eur. J.* 2010; (16) 13127-13138.
16. Lee W, Cho N, Kwon J, Ko J, Hong JI. New Organic Dye Based on a 3,6-Disubstituted Carbazole Donor for Efficient Dye-Sensitized Solar Cells. *Chem. Asian J.* 2012; 7: 343-350.
17. Hao S, Wu J, Huang Y, Lin J. Natural dyes as photosensitizers for dye-sensitized solar cell. *Sol. Energy* 2006; 80: 209-214.
18. Chang H, Wu HM, Chen TL, Huang KD, Jwo CS, Lo YJ. Dye-sensitized solar cell using natural dyes extracted from spinach and ipomoea. *J. Alloy. Compd.* 2010; 495: 606-610
19. Ortiz NMG, Maldonado IAV, Espadas ARP, Rejon GJM, Barrios JAA, Oskam G, Dye-sensitized solar cells with natural dyes extracted from achiote seeds. *Solar Energy Mater. Solar Cells* 2010; 94: 40-44
20. Zhao W, Bian W, Investigation of the structures and electronic spectra for coumarin 6 through TD-DFT calculations including PCM solvation. *J. Mol. Struct. THEOCHEM* 2007, (818) 43-49
21. Becke AD, Density-functional chemistry. III. The role of exact exchange. *J. Chem. Phys.* 1993; 8: 5648-5653.
22. Lee C, Yang W, Parr RG, Development of the Colle-Salvetti correlation-energy formula into a functional of the electron density. *Phys. Rev. B.* 1988 ;37: 785-793.

23. Opera CI, Panait P, Cimpoesu F, Ferbinteanu M, Girtu MA, Density functional theory (DFT) study of Coumarin-based dyes adsorbed on TiO<sub>2</sub> nanoclusters—applications to dye-sensitized solar cells. *Materials* 2013;6: 2372–2392
  24. Zhang CR, Liu L, Zhe JW, Jin NZ, Ma Y, Yuan LH, Zhang ML, Wu YZ, Liu ZJ, Chen HS, The role of the conjugate bridge in electronic structures and related properties of tetrahydroquinoline for dye sensitized solar cells. *Int. J. Mol. Sci.* 2013; 14: 5461–5481
  25. Abdullah MI, Janjua MRSA, Mahmood A, Ali S, Ali M, Quantum chemical designing of efficient sensitizers for dye sensitized solar cells. *Bull. Korean Chem. Soc.* 2013; 34:2093–2098.
  26. Parr RG, Donnelly RA, Levy M, Palke WE, Electronegativity: The density functional viewpoint *J. Chem. Phys.*, 1978; 68: 3801.
  27. Foresman JB, Frisch A, *Exploring Chemistry with Electronic Structure Methods*. Gaussian, Inc., Pittsburg, PA (USA), 1995.
  28. Geerlings P, Proft FD, Langenaeker W, *Conceptual Density Functional Theory* *Chem. Rev.*, 2003;103: 1793.
  29. Pauling L. *The Nature of the Chemical Bond*. Cornell University Press, Ithaca, New York, 1960
  30. Babu GA, Ramasamy P, Growth and characterization of an organic nonlinear optical material ammonium malate, *Curr. Appl. Phys.*, 2010; 10: 214,
  31. Pasquarello A, Laasonen K, Car R, Lee C, Vanderbilt D, Ab initio molecular dynamics for d - electron systems: Liquid copper at 1500 K *Phys. Rev. Lett.* 1992; 69: 1982.
  32. Fatma S, Bishnoi A, Verma AK, Synthesis, spectral analysis (FT-IR, <sup>1</sup>H NMR, <sup>13</sup>C NMR and UV–visible) and quantum chemical studies on molecular geometry, NBO, NLO, chemical reactivity and thermodynamic properties of novel 2-amino-4-(4-(dimethylamino)phenyl)-5-oxo-6-phenyl-5,6-dihydro-4H-pyrano[3,2-c]quinoline-3-carbonitrile *Journal of Molecular Structure* 2015; 1095: 112–124.
  33. Glossman-Mitnik D, *Procedia Computational Study of the Chemical Reactivity Properties of the Rhodamine B Molecule* *Computer Science* 2013; 18: 816 – 825.
  34. Zaater S, Bouchoucha A, Djebbar S, Brahimi M, Structure, vibrational analysis, electronic properties and chemical reactivity of two benzoxazole derivatives: functional density theory study. *Journal of Molecular Structure* 2016; 1123: 344–354.
-